Contagion Modeling

Chen, Yuxin* Mackey, Alan† Royston, Michael‡ Totari, Emad§

August 10, 2012

1 Introduction to contagion modeling and crowd survival

Large groups of individuals defending themselves from an attacker is a common occurance everyday. A school of fish being attacked by a shark, for example, or a herd of zebras trying to escape from a lion. Another example would be the crowd of people in the annual Running of the Bulls in Spain. The situations surrounding these crowds vary, a school of fish has a large essentially unbounded area to escape in. The herd of zebras still have an essentially unbounded area to run in, but now there are obstacles that need to be avoided. The crowd of people are running in a confined area with obstacles.

One interesting feature of crowds is that information can flow through them. This can be seen with a flock of birds flying through the air and moving as a group, or a school of fish avoiding a predator. Each individual member of the crowd is described by its position and velocity and, in addition to that, by a quantification of some emotion, such as fear, or alertness, which changes how they react to certain stimuli. For example a fish that is scared might run away from where they believe the fear is coming from. The phenomenon by which this emotion spreads among the population is called *contagion*. This is included in our models as a way to increase survival rates of individual particles.

1

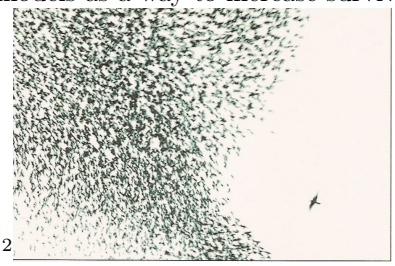

2

Previous works have spent time analyzing the movement and formation of crowds such as the formation of home territories of coyotes [7]. These works often use a continuum model to find the expected density at a given time. These continuum models have also been extended to describe the flow of people in a crowd line in [2] While the continuum model works well to capture the macroscopic qualities of crowds, it is of interest to know where the individual memebrs of the crowd are at a given time. As such a discrete model can be benefecial to capture both the macroscopic and the microscopic dynamics of crowds.

*Dalhousie University. Email: yuxinchen0612@gmail.com
†UCLA. Email: mackeya@math.ucla.edu
‡UCLA. Email: Michael@royston.com
§UCLA. Email: etota001@math.ucla.edu
[1]http://i.telegraph.co.uk/multimedia/archive/01940/overhead-crowd_1940520i.jpg
[2]http://4.bp.blogspot.com/-g1UjsJ3y4OY/TXzpRD7FRsI /AAAAAAAAAZQ/FtZSwvjlhe0/s1600/Peregrine%2526Flock.JPG

Previous studies from biology have got some natural predator-prey phenomena with advanced technology. In [3], with high-resolution sonar imaging to track the motion and interactions among sea trout and its schooling prey, juvenile Gulf menhaden, they observe that the predators prefer to attack lager groups and to impede prey from rejoining the original shool. In our study, we have set up two different predator-prey models to simulate the natural predator-prey behaviors described in this paper. The first one is to incorporate a fear field with the prey swarming system. The second one is to replace the previous fear field with the interaction terms between predator and preys in the system.

2 Bounded Room

The first scenario we wished to model was individuals escaping from a bounded room. This can simulate a fire occuring in a room, or a sheepdog in a sheep's pen[1]. To begin with we needed a room to simulate. We decided on a square room with walls of length 6 units, with a door at the top of length 0.6 units. Obstacles such as walls or pillars are placed in the room to restrict the movement of individuals and to influence how they leave the room.

2.1 The Model

Typically in an agent based model each individual particle has rules for interacting with the other particles in the simulation. In open space this model works, but once obstacles are introduced these agent-based dynamics become increasingly complicated. Now instead of only interacting with other particles, each particle needs rules for interacting with any obstacles introduced into a room. These rules can be implemented using strictly agent based dynamics, however the computations are complex. Essentially each particle wants to find an optimal path out of the room based off of the location of the other particles and any obstacles. Instead of having each particle calculate their own path, we create a field for these paths to follow.
We begin with some assumptions about how we want people to move.

Assumption 1. *There is a goal or set of goals that people want to reach.*

One example for this goal set would be the area contained within the doorway. This goal set can also be dynamic, such as the set of all points that are far from an attacker, or close to an individual. This goal set can also be part dynamic and part static.

Assumption 2. *There are regions of discomfort defined by a function g(x), s.t. if g(x)>g(x') then a person would rather move through x'.*

This assumption allows us to define high discomfort areas such as walls, obstacles, and in this specific case fear sources. If we combine these two assumptions we can generate a cost field across our domain. This cost field has a base cost of β across the entire field. This serves as a forcing term that with nothing else in the room will cause people to exit by the shortest pathwise distance to the goal set. The discomfort field is added into the cost field to discourage paths from using that area of the domain. The cost field appears as follows

$$C(x) = \beta + \gamma g(x)$$

For the purposes of our simulations β and γ are 1. The discomfort field g has four components. The first is a constant forcing term near the boundary to discourage people from being at the boundary. The second is a gaussian placed at each person and is scaled by their fear. This serves to discourage people from entering areas of the room where other people are scared. The third term is another gaussian placed at any obstacles in the room. And the fourth is a gaussian placed at any "predator" points in the room. The reason gaussians are used is because they allow for the discomfort function to scale to different sized grids.

Once this cost field has been generated, a shortest path from a person to the goal set still needs to be found. The potential function ϕ defined by the Eikonal Equation can be used to find this shortest path [9]. If ϕ is defined to be 0 in the goal set and satisfies

$$\|\nabla\phi\| = C$$

Then the shortest path for a given point follows the gradiant of ϕ at that point. Now that we have a direction for our path, we need a speed to follow the path.

Assumption 3. *The speed of any given person is density dependent. People in low density move fast, people in high density move slowely.*

Adding in this assumption allows us to put together a basic second order model for the room.

$$\begin{aligned}\frac{dx_i}{dt} =& \frac{\rho_{max}-\rho}{\rho_{max}}v_i \\ \frac{dv_i}{dt} =& (\nabla\phi(x_i) - v_i) \\ \|\nabla\phi\| =& \beta + \gamma g(x)\end{aligned}$$

Collisions are handled by a cutoff repulsion factor. When any two points are within a small distance of each other (in our simulations it was .25), both particles were pushed with a force equal to the inverse of their distance. The force was cut off at $\frac{1}{\sqrt{dt}}$ in order to avoid blow up if two points got too close in a time step. In addition for simulations requiring a predator, they are attracted to their nearest neighbor with a fixed speed.

2.2 Showing Eikonal Equation solves shortest path

Now we need to show that the solution to the Eikonal Equation $\|\nabla\phi\| = C$ can give us a shortest path. If we call Ω the domain where the individuals can move, that is, the room, and *Gamma* the goal set they want to reach, this is stated in the following result

Theorem 1. *Let Ω be any bounded connected domain and let $\Gamma \subset \Omega$. Let $\phi : \Omega \to \mathbb{R}$ such that $\phi \equiv 0$ on Γ. Then the shortest path for particle at a given point x to the goal set Γ follows the gradiant descent path of the solution to the Eikonal Equation $\|\nabla\phi\| = C$*

Proof. We follow ideas in [4]. The shortest path from any point to our goal set will be the path P that satisfies $\min_P \int_P C(x)ds$
To begin with let us parameterize our path P by $P = f(t), t \in [0,1]$. Now we wish to solve

$$\min_f \int_0^1 C(f(t))\|\dot{f}(t)\|dt = \int_0^1 I(f,\dot{f}).$$

Here $I(f,\dot{f})$ is the functional that we are trying to minimize along our path. If we show that the parametrization characterized by the gradiant descent path solves the Euler Lagrange equation for I then we have shown that it is a minimzer of I and we are done. The Euler Lagrange Equation is

$$0 = \frac{\partial I}{\partial f} - \frac{d}{dt}\left(\frac{\partial I}{\partial \dot{f}}\right) \tag{1}$$

In the case we are interested in, the right hand side of the quation reads

$$\begin{aligned}(E-L) &= \nabla C(f)\|\dot{f}\| - \frac{d}{dt}\left(C(f)\frac{\dot{f}}{\|\dot{f}\|}\right) \\ &= \nabla C(f)\|\dot{f}\| - \left[(\nabla C(f)\cdot\dot{f})\frac{\dot{f}}{\|\dot{f}\|} + C(f)\frac{\|\dot{f}\|\ddot{f} - \left(\frac{\dot{f}}{\|\dot{f}\|}\cdot\ddot{f}\right)\dot{f}}{\|\dot{f}\|^2}\right]\end{aligned}$$

To show that (E-L) is zero, and thus a solution to (1) it suffices to show that (E-L)$\cdot V = 0$ and (E-L)$\cdot V^{\perp} = 0$ for any nonzero vector V. First choose V = $(\dot{f})$ Then (E-L)$\cdot V$ reduces to

$$\begin{aligned}
&\nabla C(f)\|\dot{f}\|\dot{f} - \left[(\nabla C(f)\cdot\dot{f})\frac{\dot{f}}{\|\dot{f}\|}\dot{f} + C(f)\frac{\|\dot{f}\|\ddot{f} - \left(\frac{\dot{f}}{\|\dot{f}\|}\cdot\ddot{f}\right)\dot{f}}{\|\dot{f}\|^2}\dot{f}\right] \\
&= \nabla C(f)\|\dot{f}\|\dot{f} - \left[\nabla C(f)\|\dot{f}\|\dot{f} + C(f)\frac{\|\dot{f}\|\ddot{f}\dot{f} - \left(\frac{\dot{f}}{\|\dot{f}\|}\cdot\ddot{f}\right)\|\dot{f}\|^2}{\|\dot{f}\|^2}\right] \\
&= 0
\end{aligned}$$

Now if we let V = $(\dot{f})^{\perp}$ Then (E-L)$\cdot V$ reduces to

$$\begin{aligned}
&\nabla C(f)\|\dot{f}\|\cdot\dot{f}^{\perp} - \left[(\nabla C(f)\cdot\dot{f})\frac{\dot{f}}{\|\dot{f}\|}\dot{f}^{\perp} + C(f)\frac{\|\dot{f}\|\ddot{f} - \left(\frac{\dot{f}}{\|\dot{f}\|}\cdot\ddot{f}\right)\dot{f}}{\|\dot{f}\|^2}\dot{f}^{\perp}\right] \\
=&\dot{f}^{\perp}\cdot\nabla C(f)\|\dot{f}\| - \left[0 + C(f)\frac{\|\dot{f}\|\ddot{f}\cdot\dot{f}^{\perp} - 0}{\|\dot{f}\|^2}\right] \\
=&\dot{f}^{\perp}\cdot\nabla C(f)\|\dot{f}\| - C(f)\frac{\ddot{f}\cdot\dot{f}^{\perp}}{\|\dot{f}\|}
\end{aligned}$$

Now we need to show $\dot{f}^{\perp}\cdot\nabla C(f)\|\dot{f}\|^2 = C(f)(\ddot{f}\cdot\dot{f}^{\perp})$. Let us choose the parameterization for f such that $\dot{f} = \nabla u$ then

$$\begin{aligned}
&(\dot{f}^{\perp}\cdot\nabla C(f))\|\dot{f}\|^2 = (\nabla u^{\perp}\cdot\nabla C)C^2 \\
&= ((-u_y,u_x)\cdot\nabla\|\nabla u\|)\,(C^2) \\
&= \left((-u_y,u_x)\cdot\nabla\sqrt{u_x^2+u_y^2}\right)(C^2) \\
&= \left((-u_y,u_x)\cdot\frac{(u_xu_{xx}+u_yu_{xy},u_xu_{xy}+u_yu_{yy})}{C}\right)(C^2) \\
&= ((u_xu_{xx}+u_yu_{xy},u_xu_{yx}+u_yu_{yy})\cdot(-u_y,u_x))\,(C)
\end{aligned}$$

$$\begin{aligned}
&(\ddot{f}\cdot\dot{f}^{\perp})C = (\dot{\nabla u}\cdot\nabla u^{\perp})C \\
&= \left(\frac{d}{dt}(u_x(f(t)),u_y(f(t)))\cdot(-u_y,u_x)\right)C \\
&= \left((\nabla u_x\cdot\dot{f},\nabla u_y\cdot\dot{f})\cdot(-u_y,u_x)\right)C \\
&= (([u_{xx},u_{xy}]\cdot[u_x,u_y],[u_{yx},u_{yy}]\cdot[u_x,u_y])\cdot(-u_y,u_x))\,C \\
&= ((u_xu_{xx}+u_yu_{xy},u_xu_{yx}+u_yu_{yy})\cdot(-u_y,u_x))\,(C)
\end{aligned}$$

Since $(\dot{f}^{\perp}\cdot\nabla C(f))\|\dot{f}\|^2 = (\ddot{f}\cdot\dot{f}^{\perp})C$ for this parametrization then the E-L equation is 0, which implies that this parametrization is a minimizer of the original functional. □

2.3 Numerical Simulation

Our numerical simulation was done in both Matlab and C++. All of the a priori work to solve the Eikonal Equation and keep track of the individuals was done in Matlab while solving the Eikonal

Equation was done in C++, by a Hamiltion-Jacobi Solver by Shawn Walker [3]. The set up in matlab was based off of the work done by Treuille et al [9]. Our first attempt was based off of the work by Polymenakos et al[8] but matlab was not suited to handle their method.
To begin with we set up a square grid that covers our domain. Each node has a neighbor in each cardinal direction, North, South, East, and West. In addition each node of the grid has knowledge about which other nodes are its neighbors. We also mark each node to establish if it is in the interior of our domain or on the boundary. Each node also keeps track of the value of the cost field at its current location.
At each step of our simulation we begin by calculating the cost field at every node. The cost field has several components. First if the node is close to the boundary (within 10%) we had a forcing term to keep individuals away from the boundary. Next we add in the cost of any obstacles in the domain by adding in a gaussian to our field centered at every obstacle. In addition we add a gaussian scalled by individual's fear level at each individual. Now that we have the cost field at each point we find the average vertical and average horizontal cost at each point and store that in the node. We next find our goal set. In our situation the door was always considered a goal set, so we find which nodes are in the doorway that was labeled before. There were also conditions for the goal set such as being a certain distance from the predator when he was too close to the door. These conditions were included here. Next we run the C++ mex file on all of this to produce the solution to our Eikonal Equation. Once we have the solution at every node, we calculate the gradient at each node using matlab's gradient function.
Next we interpolate these gradients to find the gradient at each individual. We then run all of our updates for position, speed, and fear. For fear we bring each individual who is below the average closer to the average, and then apply an extra term for any fear sources from predators. Speed is done by subtracting the current speed from the interpolated field and using that as the change of speed. This causes an alignment of velocity to the field. Finally position is updated by scaling the velocity by the density at that point and using that as the change of position.

2.4 Numerical Results

Several interesting results came up during the simulations. The first was that when an obstacle was placed in front of the door there was a drastic increase in particles exit speed in comparison to placing the obstacle in the center of the room. When the fear source was placed at the door it took 100 people 22.69 seconds to exit the room. When the fear source was placed at the center of the room it took 33.19 seconds for the same people to leave the room. We believe that this is because when there is no obstacle at the door people get gridlocked trying to exit. With an obstacle people are filed out in two lines. This also agrees with the result found in Hughes /citeHughes_2002

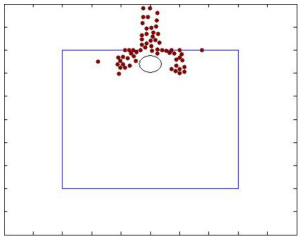

Figure 1: Obstacle at door after 15 seconds

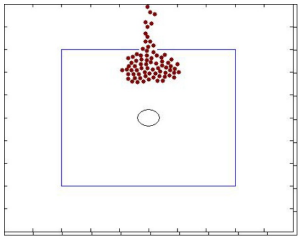

Figure 2: Obstacle in center after 15 seconds

The next interesting result was that once an attacker was added to the room. They chased the nearest

[3]http://www.mathworks.com/matlabcentral/fileexchange/24827-hamilton-jacobi-solver-on-unstructured-triangular-grids/content/HJB_Solver_Package/@SolveEikonalmex/SolveEikonalmex.m

person and turned them into a fear source when they got within 0.1 distance of them. One benefecial strategy for him was to stay at the door because people had to leave. To combat this for the people, we added a toggle that when the attacker was too close to the door the people ran away from the attacker to any point more than 2 unit distance away. The interesting part about this toggle was that this was only beneficial to the people when the attacker started farther away from the door. Here the door is located at 0,3

Attacker Start = [0,2]		Attacker Start = [0,0]		Attacker Start = [0,-2]	
Toggle	Regular	Toggle	Regular	Toggle	Regular
80.4667	80.9000	81.1667	78.6333	87.6333	81.7000

The above table represents the average of 30 trials run at points near the listed start points. Because the system is chaotic, small differences in initial data produce vastly different results. The 30 runs is to find the average at that point. Interestingly when the attacker starts near the door the peoples response to the attacker at the door doesn't change the results. However when the attacker started away from the door, having the field toggle had a large increase in survivability.

3 Unbounded Space

The goal of the project was to construct models for interacting individuals that includes the spread of emotion and how it affects their behavior. Most systems of animals have a mechanism of communication with each other to help warn fellow animals of a imminent threat and this is the idea that we wanted to be evident in the simulations.The interaction between the prey and the predator is set up for a fish based model. The prey exhibit flocking behavior amongst themselves. The predator goes after the closest prey, while the prey runs away from the nearest predator. The prey gain fear when close to the predator and this fear can spread amongst the prey which in turn increases their speed. The main goal of this part of the model is to show how contagion can help the survival of the Prey. When a predator heads towards a flock of prey, their fear increases and it spreads to the back of the flock which will prepare them for the predator. Numerous data simulations were run to see how much the contagion helped increase the survival rate of the prey.

• **Model for the Predator**

$$\frac{dx_i}{dt} = v_{x_i}$$
$$\frac{dv_{x_i}}{dt} = -v_{x_i} + A\frac{y_j - xi}{|y_j - x_i|} \; s.t. \; |y_j - x_i| = \min_{1\le s\le n} |y_s - x_i|$$

• **Model for the Prey**

$$\frac{dy_i}{dt} = (1 + 2q_{y_i})v_{y_i}$$
$$\frac{dv_{y_i}}{dt} = -v_{y_i} + \chi_{\{r\le 1\}}(|y_i - x_j|)\frac{y_i - x_j}{|y_i - x_j|^{1+2q_{y_i}}} + \chi_{\{r>1\}}(|y_i - x_j|)\frac{y_i - x_j}{|y_i - x_j|^2} + \frac{1}{n}\sum_{j\neq i} F(|y_j - y_i|)\frac{y_i - y_j}{|y_i - y_j|}$$
$$s.t. \; |y_i - x_j| = \min_{1\le s\le m} |y_i - x_s|$$
$$\frac{dq_{y_i}}{dt} = \frac{B}{n}\sum_{j\neq i}\frac{q_{y_j} - q_{y_i}}{\epsilon + |y_i - y_j|^2} + \frac{1}{D}\sum_{|x_j - y_i|\le C}\frac{\frac{1}{2} - q_{y_j}}{|x_j - y_i|} + \frac{1}{E}\sum_{|x_j - y_i|>C}(-q_{y_i})$$
$$F(r) = \frac{1}{r} - r$$

3.1 Description of the Model

The model is a 2nd order model(i.e. incorporates position, velocity, and acceleration). Let m be the number of prey and n be the number of predators then we have system of (5m + 4n) ODEs.

• **Predator Terms**

$$\frac{dx_i}{dt} = v_{x_i}$$

This term says that the change in position is the velocity.

$$\frac{dv_{x_i}}{dt} = -v_{x_i} + A\frac{y_j - xi}{|y_j - x_i|} \; s.t. \; |y_j - x_i| = \min_{1 \le s \le n} |y_s - x_i|$$

This term includes a dampening velocity term which could be considered a drag term and the second term says that each predator goes after the closest prey.

• **Prey Terms**

$$\frac{dy_i}{dt} = (1 + 2q_{y_i})v_{y_i}$$

The way the Prey moves depends on how high its fear is.

$$\frac{dv_{y_i}}{dt} = -v_{y_i} + \chi_{\{r \le 1\}}(|y_i - x_j|)\frac{y_i - x_j}{|y_i - x_j|^{1+2q_{y_i}}} + \chi_{\{r > 1\}}(|y_i - x_j|)\frac{y_i - x_j}{|y_i - x_j|^2}$$

$$+\frac{1}{n}\sum_{j \neq i} F(|y_j - y_i|)\frac{y_i - y_j}{|y_i - y_j|} s.t. \; |y_i - x_j| = \min_{1 \le s \le m} |y_i - x_s|$$

$$F(r) = \frac{1}{r} - r$$

The first term is again a dampening velocity term. The next two terms describe the behaviour of the preys interaction with the predator. Each prey run away from the nearest predator, and depending on how close they are they behave differently. The fourth term is a aggregation term for the prey. It has a newtonian potential, so if the particles are far away they attract each other and if they are close they repel, which allows for some optimal distance where they are happy to be from each other. This makes it so they form some ball shape. The reason we decided to allow the prey to have a full cone of vision is because of the lateral line on fish, it allows them to essentially see in all directions.

$$\frac{dq_{y_i}}{dt} = \frac{B}{n}\sum_{j \neq i} \frac{q_{y_j} - q_{y_i}}{\epsilon + |y_i - y_j|^2} + \frac{1}{D}\sum_{|x_j - y_i| \le C} \frac{\frac{1}{2} - q_{y_j}}{|x_j - y_i|} + \frac{1}{E}\sum_{|x_j - y_i| > C} (-q_{y_i})$$

This last ODE describes how the fear of each prey can increase or decrease. The first term introduces the spread of fear among the prey. The next two terms say that if the prey is within a certain distance of the predator then their fear increases but if they are outside of that distance then their fear decreases due to a dampening velocity term.

4 Results

After running numerous simulations using the forward euler method in matlab with and without considering the contagion phenomenon, the dynamics of the prey behavior was much different in the two cases. We ran the simulations with low number of predators and thousands of prey. The prey were more adept to survive the attack from the pedator. Using the number of survived prey as a metric, the comparison from a system where the contagion effect is present to another one without it shows that the survival rate is much higher in the case of the contagion. Currently we are trying to understand the best formation for the predators in order to attack the prey, after many numerical

simulations for two predators it is best for their angle of separation to be between 90 and 140 degrees apart.
Here we plot a 30 run average of the angle of seperation vs. the number of prey that survived

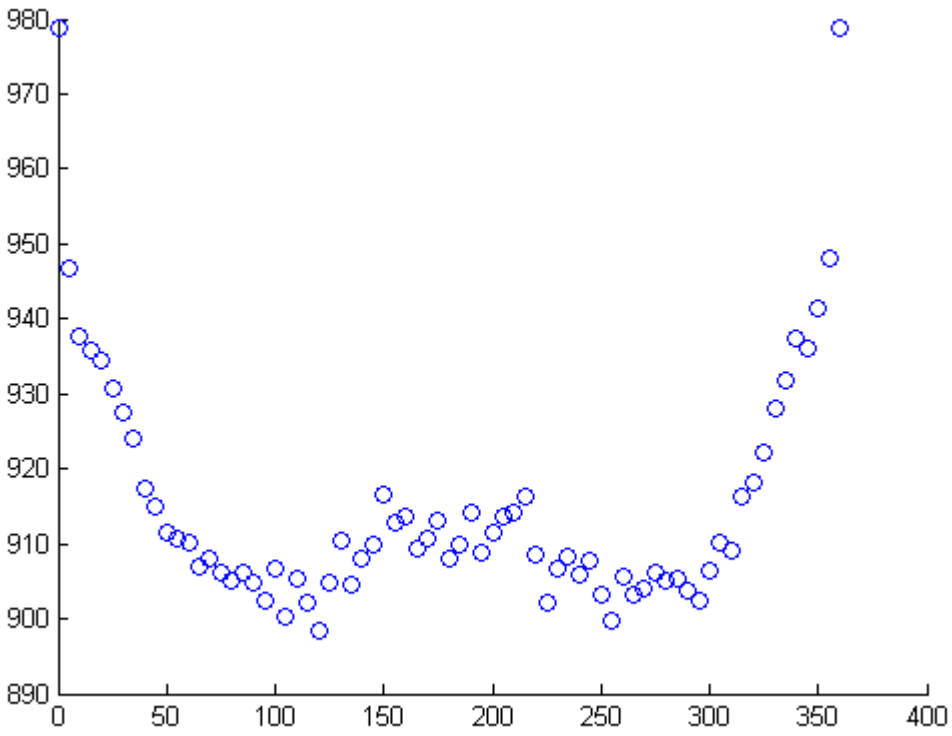

5 Predator and Prey Model in 2D

Aggregation models of single species with attractive-repulsive force laws have been broadly studied. In [6], the stability of ring pattern at the steady state has been analyzed, and [5] studies singular perturbations off lower-dimensional steady states.
In our study, we use similar methods but add a predator-prey interaction term into the aggregation model of the prey. The model includes N many preys and one predator. We call $F(r)$ the force term which will cause different patterns at the steady state. $H(r)$ and $I(r)$ are the interaction terms between prey and predator in the prey's system and predator's system, respectively. The second order model for the prey is:

$$\frac{dv_j}{dt} = -v_j + \frac{1}{N}\sum_{k=0,k\neq j}^{N-1} F(\|x_j - x_k\|)\frac{x_j - x_k}{\|x_j - x_k\|} + H(\|x_j - z\|)(x_j - z), \tag{2}$$

$$\frac{dx_j}{dt} = v_j \qquad j = 1...N, \tag{3}$$

where x_j's and v_j's denote the position and velocity of each particle j, respectively. And the second order model for the predator is:

$$\frac{du}{dt} = -u + \frac{c}{N}\sum_{j=1}^{N} I(\|x_j - z\|)(x_j - z), \tag{4}$$

$$\frac{dz}{dt} = u, \tag{5}$$

where z and u denote the position and velocity of the predator, respectively, and c is a parameter that should be chosen reasonably so that the numerical result agrees with the real phenomenon.

5.1 Stability analysis of the steady state

In numerics, we notice that different potential functions $F(r)$, $H(r)$ and $I(r)$ will give different equilibria stability phenomena. We start with the easy case, where only the predator is perturbed and the preys are fixed on the ring. Next we perturb both the predator and preys in a first order model.

• Radius of the ring pattern at steady state
We consider the prey particles locate at an equally spaced ring and the predator locates at the center of the ring at the steady state. For $j = 1...N$, taking $x_j = Re^{\frac{2\pi ij}{N}}$, $z = \mathbf{0}$ and plugging into equations (2) and (3) give:

$$0 = \frac{1}{N}\sum_{k=1}^{N-1} F\left(2R\sin\left(\frac{\pi k}{N}\right)\right)\frac{1 - exp(\frac{2\pi ik}{N})}{2R\sin(\frac{\pi k}{N})} + RH(R) \tag{6}$$

So at the steady state, the radius R has to satisfy equation (6).

• Perturbation of the predator with the ring of fixed N prey
We start with the simple case when the prey is fixed on the equally spaced ring and in particular, take $F(r) = r^{0.5} - r^2$, $H(r) = \frac{1}{r^2}$, and add a small perturbation to the predator, $z = \mathbf{0} + Be^{\lambda t}$. Then $\dot{z} = u = B\lambda e^{\lambda t}$ and $\dot{u} = A\lambda^2 e^{\lambda t}$. Plugging these into the predator velocity equations (2) and (3) and linearizing the sum term gives:

$$\lambda^2 + \lambda + \frac{N}{R^q + 1} - \frac{NqR^q}{2(R^q + 1)^2} = 0. \tag{7}$$

Solving the quadratic equation, we get

$$\lambda_{1,2} = \frac{-1 \pm \sqrt{1 + \frac{2N(qR^q - 2R^q - 2)}{(R^q+1)^2}}}{2},$$

where R satisfies equation (6).

• Perturbation of the ring with N prey particles and one predator
Only consider the perturbation of predator is not enough in reality, but the stability analysis of the second order model with perturbation of both predator and prey is more complicated, so we consider the first order prey model

$$\frac{dx_j}{dt} = \frac{1}{N}\sum_{k=0,k\neq j}^{N-1} F(\|x_j - x_k\|)\frac{x_j - x_k}{\|x_j - x_k\|} + H(\|x_j - z\|)(x - z). \tag{8}$$

Taking $x_j = Re^{\frac{2\pi ij}{N}}(1+\phi_j e^{\lambda t})$, $z = Be^{\lambda t}$, with $0 < \|\phi_j\|, \|A\| \ll 1$ and plugging them into the first order model equation gives:

$$\lambda R e^{\frac{2\pi ij}{N}}\phi_j e^{\lambda t} = \frac{1}{N}\sum_{k=0,k\neq j}^{N-1} F(\|a+\epsilon\|)\frac{a+\epsilon}{\|a+\epsilon\|} + H(\|b+\delta\|)(b+\delta), \tag{9}$$

where $a = R(e^{\frac{2\pi ij}{N}} - e^{\frac{2\pi ik}{N}})$, $\epsilon = Re^{\lambda t}(e^{\frac{2\pi ij}{N}}\phi_j - e^{\frac{2\pi ik}{N}}\phi_k)$, $b = Re^{\frac{2\pi ij}{N}}$, and $\delta = e^{\lambda t}(R\phi_j e^{\frac{2\pi ij}{N}} - B)$. Using Taylor expansion to the first order, we get:

$$\begin{aligned}\lambda\phi_j = &\frac{1}{N}\sum_{k=0,k\neq j}^{N-1}\left[G_+\left(\frac{\pi(k-j)}{N}\right)\left(\phi_j - \phi_k e^{\frac{2\pi i(k-j)}{N}}\right) + G_-\left(\frac{\pi(k-j)}{N}\right)\left(\bar{\phi}_j - \bar{\phi}_k e^{\frac{2\pi i(k-j)}{N}}\right)\right]\\ &+ \frac{H'(R)}{2}\left(R\phi_j - Be^{\frac{-2\pi ij}{N}} + R\bar{\phi}_j - \bar{B}e^{\frac{2\pi ij}{N}}\right) + H(R)\left(\phi_j - \frac{A}{R}e^{\frac{-2\pi ij}{N}}\right)\end{aligned} \tag{10}$$

where $G_\pm(\theta) = \frac{1}{2}\left[F'(2R|\sin(\theta)|) \pm \frac{F(2R|\sin(\theta)|)}{2R|\sin(\theta)|}\right]$.
Next we take $\phi_j = b_+ e^{\frac{2m\pi ij}{N}} + b_- e^{\frac{-2m\pi ij}{N}} + Be^{\frac{2\pi ij}{N}} + \bar{B}e^{\frac{-2\pi ij}{N}}$. Plugging it into equation (10) and collecting the common exponential terms, we get:

$$LHS(10) = \lambda(b_+ e^{\frac{2mij\pi}{N}} + b_- e^{-\frac{2mij\pi}{N}} + Be^{\frac{2\pi ij}{N}} + \bar{B}e^{-\frac{2\pi ij}{N}}); \tag{11}$$

$$\begin{aligned}RHS(10) = &\frac{1}{N}\sum_{l=1}^{N}\left\{G_+\left(\frac{\pi l}{N}\right)\left[e^{\frac{2mij\pi}{N}}b_+(1-e^{\frac{2(m+1)il\pi}{N}}) + e^{-\frac{2mij\pi}{N}}b_-(1-e^{\frac{2(-m+1)il\pi}{N}}) + Be^{\frac{2\pi ij}{N}}(1-e^{\frac{4\pi il}{N}})\right]\right.\\ &\left. G_-\left(\frac{\pi l}{N}\right)\left[e^{\frac{2mij\pi}{N}}b_-(e^{\frac{2mil\pi}{N}} - e^{\frac{2\pi il}{N}}) + e^{-\frac{2mij\pi}{N}}b_+(e^{-\frac{2mil\pi}{N}} - e^{\frac{2\pi il}{N}}) + \bar{B}e^{-\frac{2\pi ij}{N}}(e^{-\frac{2\pi il}{N}} - e^{\frac{2\pi il}{N}})\right]\right\}\\ &+ e^{\frac{2mij\pi}{N}}\left[\frac{H'(R)R}{2}(b_+ + b_-) + b_+H(R)\right] + e^{-\frac{2mij\pi}{N}}\left[\frac{H'(R)R}{2}(b_+ + b_-) + b_-H(R)\right]\\ &+ e^{\frac{2ij\pi}{N}}\left[\frac{H'(R)}{2}(2RB - \bar{B}) + BH(R)\right] + e^{-\frac{2ij\pi}{N}}\left[\frac{H'(R)}{2}(2R\bar{B} - B) + H(R)\left(\bar{B} - \frac{B}{R}\right)\right]\end{aligned} \tag{12}$$

The equation can be rewritten as the eigenvalue problem:

$$\lambda\begin{bmatrix} b_+ \\ b_- \\ B \\ \bar{B}\end{bmatrix} = \begin{bmatrix} I_1(m) & I_2(m) & 0 & 0 \\ I_2(m) & I_1(-m) & 0 & 0 \\ 0 & 0 & K_1 & K_2 \\ 0 & 0 & J_1 & J_2\end{bmatrix}\begin{bmatrix} b_+ \\ b_- \\ B \\ \bar{B}\end{bmatrix} \tag{13}$$

where

$$
\begin{aligned}
I_1(m) =& \frac{1}{N}\sum_{l=1}^{N} G_+\left(\frac{\pi l}{N}\right)\left(1-e^{\frac{2(m+1)il\pi}{N}}\right)+\frac{H'(R)R}{2}+H(R),\\
I_2(m) =& \frac{1}{N}\sum_{l=1}^{N} G_-\left(\frac{\pi l}{N}\right)\left(e^{\frac{2mil\pi}{N}}-e^{\frac{2\pi il}{N}}\right)+\frac{H'(R)R}{2},\\
K_1 =& \frac{4}{N}\sum_{l=1}^{N/2} G_+\left(\frac{\pi l}{N}\right)\sin^2\left(\frac{2\pi l}{N}\right)+RH'(R)+H(R),\\
K_2 =& -\frac{H'(R)}{2},\\
J_1 =& -\frac{H'(R)}{2}-\frac{H(R)}{R},\\
J_2 =& RH'(R)+H(R).
\end{aligned}
$$

• Constant density within the annulus at the steady state of first order model in 2D
We will show that the solution of the system has the form of an annulus of uniform density at the steady state under certain conditions of $H(r)$, which is the interaction term of prey and predator in the prey system. For simplicity, we take $f(r) = F(r)/r$, where F is taken to be Newtonian potential, i.e. $F(r) = \frac{1}{r} - r$.
Take $N \to \infty$, then the system becomes:

$$\rho_t(x,t) + \bigtriangledown_x \cdot (v(x)\rho(x,t)) = 0; \tag{14}$$

$$
\begin{aligned}
v(x) &= \int_{\mathbb{R}^2} f(\|x-y\|)(x-y)\rho(y)dy + H(\|x-z\|)(x-z)\\
&= \int_{\mathbb{R}^2} [\bigtriangledown_x ln\|x-y\| - Id_2(x-y)]\rho(y)dy + H(\|x-z\|)(x-z),
\end{aligned} \tag{15}
$$

where Id_2 denotes the 2×2 identity matrix and $\rho(x,t)$ denotes the density of the prey particles.
The following proposition describes the phenomenon and we will show it by method of characteristics.

Proposition 1. *Let $D \subset \mathbb{R}^2$ be the annulus whose inner radius and outer radius are r and R, respectively. The system (15) has a steady state for which $\rho(x)$ is constant inside D and is 0 outside D under the condition that $H(r) = \frac{1}{r^2}$ or constant and.*

Proof. We use the method of characteristics:

$$
\begin{aligned}
\frac{dx}{dt} &= v;\\
\frac{d\rho}{dt} &= -(\nabla\cdot v)\rho.
\end{aligned}
$$

So

$$
\begin{aligned}
\nabla_x \cdot v &= \int_{\mathbb{R}^2} \{\Delta_x ln\|x-y\| - \nabla_x\cdot[Id_2(x-y)]\}\rho(y)dy + \nabla_x\cdot[H(\|x-z\|)(x-z)]\\
&= \int_{\mathbb{R}^2} [2\pi\delta(x-y)-2]\rho(y)dy + \nabla_x\cdot[H(\|x-z\|)(x-z)]\\
&= 2\pi\rho(x) - 2M + \nabla_x\cdot[H(\|x-z\|)(x-z)],
\end{aligned} \tag{16}
$$

where the mass $M = \int_{\mathbb{R}^2}\rho(y)dy$ is conserved.

Hence $\nabla_x \cdot H(\|x-z\|)(x-z)$ has to be constant so that $\rho(x)$ is independent of the position along the characteristic curves. So either $H(r) = \frac{1}{r^2}$ or $H(r)$ is constant and

$$\frac{d\rho}{dt} = \{2M - 2\pi\rho - \nabla_x \cdot [H(\|x-z\|)(x-z)]\}\rho. \tag{17}$$

Suppose that the initial conditions are:

$$\rho(x,0) = \begin{cases} \rho_0, & x \in D_0 \\ 0, & x \notin D_0 \end{cases}$$

where D_0 is some closed set. Hence $\rho(x,t)$ is the solution for the ODE (17) with the initial condition, $\rho(0) = \rho_0$. And ρ goes to $[2\pi M - \nabla_x \cdot [H(\|x\|)x]](2\pi)^{-1}$ as $t \to \infty$.
At the steady state, on the boundary of the domain $D(t)$, $v(x) = 0$. Using this fact, we continue to compute the inner radius r.

$$\begin{aligned} v(x) &= \int_{D(t)} \left[\frac{x-y}{\|x-y\|^2} - Id_2(x-y)\right]\rho(y,t)dy + H(\|x-z\|)(x-z) \\ &= \rho(t)\int_{D(t)} \frac{x-y}{\|x-y\|}dy - x|D(t)|\rho(t) + H(\|x-z\|)(x-z) \\ &= \pi\rho(t)x\left(1 - \frac{r^2}{\|x\|^2}\right) - x|D(t)|\rho(t) + H(\|x-z\|)(x-z) \end{aligned}$$

.
And since the velocity on the boundary should be 0 at steady state, so

$$\pi\rho(t)x\left(1 - \frac{r^2}{\|x\|^2}\right) - x|D(t)|\rho(t) + H(\|x-z\|)(x-z) = 0. \tag{18}$$

$z = 0$ is a steady state for the predator, so equation (18) becomes

$$\pi\rho(t)\left(1 - \frac{r^2}{\|x\|^2}\right) - |D(t)|\rho(t) + H(\|x\|) = 0. \tag{19}$$

On the other hand, by the fact that at the steady state, $\nabla_x \cdot v = 0$, we get $\rho = \frac{2M - \nabla_x \cdot H(\|x\|)x}{2\pi}$ and $\nabla_x \cdot H(\|x\|)x$ is constant. Hence

$$M = \int_{D(t)} \rho(y)dy = \rho|D(t)| = \frac{2\pi M - \nabla_x \cdot H(\|x\|)x}{2\pi}|D(t)|.$$

Therefore,

$$\begin{aligned} |D(t)| =& \frac{2\pi M}{2M - \nabla_x \cdot H(\|x\|)x} \\ =& \pi(R^2 - r^2) \end{aligned} \tag{20}$$

Solving equations (19) and (20) will give the inner radius and outer radius of the annulus at steady state. □

Taking $H(r) = \frac{1}{r^2}$, then we have $\rho = M/\pi$ inside the annulus at steady state. Thus from equation (20), $R^2 = r^2 + 1$. Additionally, solving equations (19) and (20) gives $r = 1$ and $R = \sqrt{2}$, which agrees with the numerical results shown in the figure below. Figure 3 demonstrates the steady state of 1500 preys and 1 predator(in red) in the form of an annulus with inner radius 1 and outer radius 1.4 approximately. Figure 4 demonstrates the annulus with 200 preys and 1 predator(in red) and results are very close to analytic results.

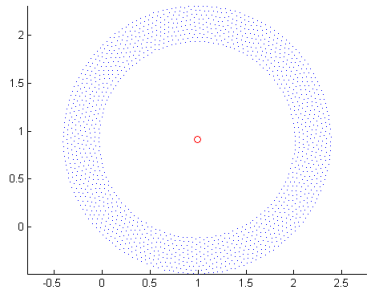

Figure 3: $H(r) = \frac{1}{r^2}$, 1500 particles

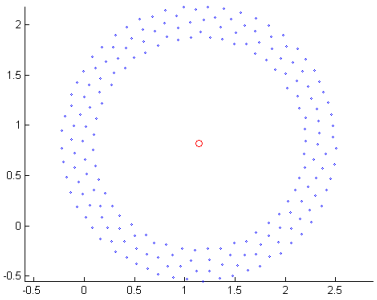

Figure 4: $H(r) = \frac{1}{r^2}$, 200 particles

6 Conclusion

We have derived a model to simulate individuals exiting a room using the Eikonal Equation. This allows us to easily insert obstacles and have individuals react to them. We have also shown that the Eikonal Equation gives us the shortest path out of the room. In the future we would like to speed up our implementation of our simulation. In addition we would like to further explore the results of putting an obstacle in front of the door to cause of speed up of exit speed

We have constructed a realistic predator prey model that incorporates fear. The fear is an important factor in the survival of prey. In the future we would like to do more analysis of how multiple predators affect the system in 3d.

We have given the eigenvalue problem set-up for the stability analysis of first order prey system, in the future, the numerical verification will be given with taking particular potential functions $F(r)$, $H(r)$ and $I(r)$. Additionally, the similar method will be used to analyze the stability of first order predator system and furthermore, the simplest first order model will be extended to second order model.

We have shown that under the condition of $H(r)$ is either $\frac{1}{r^2}$ or constant, the prey system will have an equilibrium in the form of a uniform density annulus with given inner and outer radii. In the future, we would like to study how the swarming is evolved by the predator numerically.

References

[1] Rinaldo Colombo and Magali LÃľcureux-Mercier. An analytical framework to describe the interactions between individuals and a continuum. *Journal of Nonlinear Science*, 22:39–61, 2012. 10.1007/s00332-011-9107-0.

[2] Rinaldo M. Colombo, Mauro Garavello, and Magali LÃľcureux-Mercier. Non-local crowd dynamics. *Comptes Rendus Mathematique*, 349(13âĂŞ14):769 – 772, 2011.

[3] Nils Olav Handegard, Kevin M Boswell, Christos C Ioannou, Simon P Leblanc, Dag B TjÃÿstheim, and Iain D Couzin. The dynamics of coordinated group hunting and collective information transfer among schooling prey. *Current Biology*, pages 1–5, 2012.

[4] R Kimmel and J Sethian. Optimal algorithm for shape from shading and path planning. *Journal of Mathematical Imaging and Vision*, 14(3):237–244, 2001.

[5] T. Kolokolnikov, Y. Huang, and M. Pavlovski. Singular patterns for an aggregation model with a confining potential. to appear.

[6] Theodore Kolokolnikov, Hui Sun, David Uminsky, and Andrea L. Bertozzi. Stability of ring patterns arising from two-dimensional particle interactions. *Phys. Rev. E*, 84:015203, Jul 2011.

[7] P.R. Moorcoft, M. A. Lewis, and R. L. Crabtree. Mechanistic home range models capture spatial patterns and dynamics of coyote territories in yellowstone. *Proceedings of the Royal Society B*, 273(1594):1651–1659, july 2006.

[8] L C Polymenakos, D P Bertsekas, and J N Tsitsiklis. Implementation of efficient algorithms for globally optimal trajectories. *IEEE Transactions on Automatic Control*, 43(2):577–579, 1998.

[9] Adrien Treuille, Seth Cooper, and Zoran Popović. Continuum crowds. *ACM Trans. Graph.*, 25(3):1160–1168, July 2006.